10440 *Biochemistry* **2010,** *49,* 10440–10448
DOI: 10.1021/bi1016099

BIOCHEMISTRY
including biophysical chemistry & molecular biology
*Article*

# Mechanistic Studies of the Yeast Polyamine Oxidase Fms1: Kinetic Mechanism, Substrate Specificity, and pH Dependence[†]

Mariya S. Adachi, Jason M. Torres, and Paul F. Fitzpatrick*

*Department of Biochemistry, University of Texas Health Science Center, San Antonio, Texas 78229, United States*

*Received October 5, 2010; Revised Manuscript Received November 5, 2010*

ABSTRACT: The flavoprotein oxidase Fms1 from *Saccharomyces cerevisiae* catalyzes the oxidation of spermine and $N^1$-acetylspermine to yield spermidine and 3-aminopropanal or *N*-acetyl-3-aminopropanal. The kinetic mechanism of the enzyme has been determined with both substrates. The initial velocity patterns are ping-pong, consistent with reduction being kinetically irreversible. Reduction of Fms1 by either substrate is biphasic. The rate constant for the rapid phase varies with the substrate concentration, with limiting rates for reduction of the enzyme of 126 and 1410 $s^{-1}$ and apparent $K_d$ values of 24.3 and 484 $\mu$M for spermine and $N^1$-acetylspermine, respectively. The rapid phase is followed by a concentration-independent phase that is slower than turnover. The reaction of the reduced enzyme with oxygen is monophasic, with a rate constant of 402 $mM^{-1}$ $s^{-1}$ with spermine at 25 °C and 204 $mM^{-1}$ $s^{-1}$ with $N^1$-acetylspermine at 4 °C and pH 9.0. This step is followed by rate-limiting product dissociation. The $k_{cat}/K_{amine}$−pH profiles are bell-shaped, with an average p$K_a$ value of 9.3 with spermine and p$K_a$ values of 8.3 and 9.6 with $N^1$-acetylspermine. Both profiles are consistent with the active forms of substrates having two charged nitrogens. The pH profiles for the rate constant for flavin reduction show p$K_a$ values of 8.3 and 7.2 for spermine and $N^1$-acetylspermine, respectively, for groups that must be unprotonated; these p$K_a$ values are assigned to the substrate N4. The $k_{cat}/K_{O_2}$−pH profiles show p$K_a$ values of 7.5 for spermine and 6.8 for $N^1$-acetylspermine. With both substrates, the $k_{cat}$ value decreases when a single residue is protonated.

Polyamines are essential for the growth and function of normal cells. The common polyamines putrescine, spermidine, and spermine are widely distributed in biological systems, not only as free bases but also as alkylated or acylated conjugates with sugars, steroids, phospholipids, fatty acids, and peptides. Because polyamines interact with multiple macromolecules, they affect a variety of cellular processes, such as cell growth, differentiation, and death (*1*−*3*). As a result, the biosynthetic pathway for formation of polyamines has been a target for the development of anticancer drugs (*4*). In comparison, the enzymes involved in polyamine catabolism have received much less attention (*5*). In mammalian cells, catabolism of spermine can be initiated by the action of one of two enzymes. Acetylation of spermine by spermidine/spermine $N^1$-acetyltransferase forms $N^1$-acetylspermine (Scheme 1). This can be exported from the cell or oxidized by the peroxisomal flavoprotein polyamine oxidase (PAO)[1] to spermidine and *N*-acetyl-3-aminopropanal (*6*). A further round of acetylation and oxidation by the same enzymes yields putrescine and 3-aminopropanal. Alternatively, the inducible flavoenzyme spermine oxidase (SMO) can oxidize spermine directly to spermidine and 3-aminopropanal (*7*−*9*). *Saccharomyces cerevisiae* also contains a flavoenzyme, Fms1, capable of oxidizing spermine and $N^1$-acetylspermine (Scheme 2) (*10*, *11*). The 3-aminopropanal produced by Fms1 is oxidized further to $\beta$-alanine, a precursor of pantothenic acid (*10*, *11*). Spermidine is required for formation of the modified amino acid hypusine in yeast eIF5A (*12*) and helps protect the yeast cell from oxidative stress (*13*). Plant cells also contain a flavoenzyme capable of oxidizing polyamines (*14*). In contrast to the animal enzymes, plant polyamine oxidases oxidize the *endo* C−N bond, forming 1,3-diaminopropane and *N*-(3-aminopropyl)-4-aminobutanal from spermine.

Scheme 1

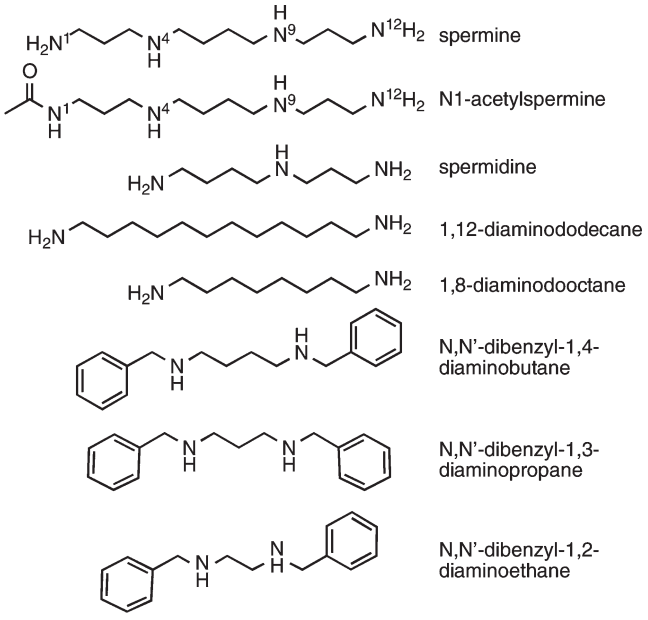


[†]This work was supported in part by National Institutes of Health Grant GM058698.

*To whom correspondence should be addressed: Department of Biochemistry, University of Texas Health Science Center, San Antonio, TX 78229. Phone: (210) 567-8264. Fax: (210) 567-8778. E-mail: fitzpatrick@biochem.uthscsa.edu.

[1]Abbreviations: MAO, monoamine oxidase; SMO, spermine oxidase; PAO, polyamine oxidase; Ni-NTA, nickel-nitrilotriacetic acid.

 Published on Web 11/10/2010 

Scheme 2

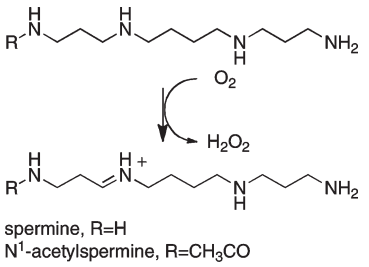


The mammalian enzymes PAO and SMO differ by 2−3 orders of magnitude in their relative preferences for $N^1$-acetylspermine versus spermine (*8*, *15*−*17*), in line with their roles in the cell. In addition, the pH optimum of PAO is more basic than that of SMO, consistent with the higher pH within peroxisomes than in the cytoplasm (*18*); the $k_{cat}/K_m$ values for spermine and $N^1$-acetylspermine as substrates for PAO have pH maxima of 10−10.5, while the $k_{cat}/K_m$ value with spermine as the substrate for SMO is highest at pH 8.3 (*16*, *17*). This difference reflects the preferences of these two enzymes for different forms of the substrate. PAO is active on the singly charged forms of polyamines, while SMO prefers polyamines with three positive charges. The structural basis for the differences is not known, because no structures are available of a mammalian PAO or SMO. Structures of Fms1 (*19*) and maize polyamine oxidase (*20*) are available. These show that these two proteins have overall structures similar to that of the monoamine oxidase (MAO) family of flavoproteins; this family also includes MAO A and B, the lysine-specific demethylase LSD1, and L-amino acid oxidases. While the levels of sequence identity between either mammalian enzyme and Fms1 or maize PAO are only ~20%, this is enough to assign both to the MAO structural family (*21*, *22*).

Because Fms1 catalyzes the same reaction as PAO and SMO, its structure serves as the best current model for understanding the structural basis for the different specificities of PAO and SMO. However, to date there has been little mechanistic study of Fms1 to guide interpretation of the relationship between structure and specificity. We describe here mechanistic studies of Fms1 using both steady-state and rapid-reaction kinetic methods and analysis of the effects of pH on the kinetic parameters. The results provide insight into the mechanism of amine oxidation by Fms1 and the basis for the differences in substrate specificity among Fms1, PAO, and SMO.

## MATERIALS AND METHODS

*Materials*. Spermine and spermidine trihydrochloride were purchased from Acros Organics (Geel, Belgium). $N^1$-Acetylspermine, 1,12-diaminododecane, 1,8-diaminooctane, *o*-dianisidine, horseradish peroxidase (72 purpurogalin units/mg), and glucose oxidase were from Sigma-Aldrich (Milwaukee, WI). *N*,*N*′-Dibenzyl-1,4-diaminobutane, *N*,*N*′-dibenzyl-1,3-diaminopropane, and *N*,*N*′-dibenzyl-1,2-diaminoethane were from Prime Organics (Woburn, MA). The pET28-based pJWL94 vector encoding His-tagged Fms1 (*11*) was kindly provided by R. Sternglanz (State University of New York, Stony Brook, NY). *Escherichia coli* BL21(DE3) Codon$^+$ RIL competent cells were from Stratagene (Santa Clara, CA). The nickel-nitrilotriacetic acid (Ni-NTA) agarose resin was purchased from Invitrogen (Carlsbad, CA).

*Expression and Purification of Fms1*. The expression and purification of Fms1 were based on the protocol described by Landry and Sternglanz (*11*). The pJWL94 vector encoding Fms1 was transformed into *E. coli* BL21(DE3) Codon$^+$ RIL cells. For the growth of Fms1, a single colony of *E. coli* (pJWL94) was used to inoculate a 60 mL culture of LB containing 25 μg/mL kanamycin and 20 μg/mL chloramphenicol. After overnight growth at 37 °C, four flasks containing 1 L of LB (25 μg/mL kanamycin and 20 μg/mL chloramphenicol) were inoculated with 10 mL each of the overnight culture. The cultures were incubated at 37 °C until the $A_{600}$ reached a value of 0.6−0.8. At this point, isopropyl β-D-thioglucanopyranoside (final concentration of 0.2 mM) was added to each flask and the temperature was decreased to 18 °C. After incubation for an additional 16 h, the cells were harvested by centrifugation at 5000*g* for 30 min at 4 °C. The cell paste was resuspended in 50 mM HEPES (pH 8.0), 10% glycerol, 2 μM pepstatin, 2 μM leupeptin, 0.1 mM NaCl, 100 μg/mL phenylmethanesulfonyl fluoride, and 100 μg/mL lysozyme and lysed by sonication. After the lysate was centrifuged at 22400*g*, the supernatant was loaded onto a 20 mL Ni-NTA column equilibrated with the same buffer. The protein was eluted with a linear gradient from 100 to 200 mM imidazole in 30 column volumes of the same buffer. Fractions containing Fms1 were pooled and concentrated using 30K Amicon Ultra Centrifugal filters. The purified protein was dialyzed against three changes of the buffer. The resulting protein sample was centrifuged at 22400*g* for 30 min at 4 °C to remove precipitated protein and stored with 10% glycerol at −80 °C.

*Extinction Coefficient of Fms1*. Five volumes of 10 M urea was added to 1 volume of enzyme in 50 mM HEPES and 10% glycerol (pH 8.0). Any precipitated protein was removed by centrifugation for 5 min at 14000*g*, and the visible absorbance spectrum of the supernatant was recorded. The change in absorbance between the enzyme-bound FAD and the free FAD after denaturation gave an extinction coefficient of 11.7 $mM^{-1}$ $cm^{-1}$ at 458 nm for the flavin in Fms1 based on the extinction coefficient of FAD of 11.3 $mM^{-1}$ $cm^{-1}$ (*23*). This value was used to determine the enzyme concentration.

*Assays*. Fms1 activity was typically determined in air-saturated buffer containing 10% glycerol by following oxygen consumption at 25 °C with a Yellow Springs Instrument model 5300 biological oxygen monitor using 0.5 μM Fms1. Buffers were 200 mM Tris-HCl from pH 7.0 to 8.75, 200 mM CHES from pH 9.0 to 9.75, and 200 mM CAPS from pH 10.1 to 10.5. Substrate concentrations were from 50 to 600 μM for spermine, $N^1$-acetylspermine, and *N*,*N*′-dibenzyl-1,3-diaminopropane and from 0.1 to 3.0 mM for *N*,*N*′-dibenzyl-1,4-diaminobutane and spermidine. $K_{is}$ and $K_{ii}$ values for 1,12-diaminododecane, 1,8-diaminooctane, and *N*,*N*′-dibenzyl-1,2-diaminoethane were determined with spermine as the substrate; the concentrations of spermine and the inhibitors were varied from 0.1 to 2.0 mM and from 0 to 5.0 mM, respectively. The $k_{cat}$ value for $N^1$-acetylspermine at 4 °C was determined using a coupled assay that measured $H_2O_2$ production. The reaction mixture contained ~45 nM Fms1, ~100 nM horseradish peroxidase, 76 μM *o*-dianisidine, and 500 μM $N^1$-acetylspermine. The rate was calculated from the increase in absorbance at 436 nm, using an extinction coefficient of 8.31 $mM^{-1}$ $cm^{-1}$. For assays not performed in air-saturated buffer, the appropriate $O_2/N_2$ mixture was bubbled into the cell of the oxygen electrode for 10 min prior to the reaction being started via the addition of enzyme.

*Rapid-Reaction Kinetics*. Rapid-reaction kinetic measurements were performed with an Applied Photophysics SX-20MV

stopped-flow spectrophotometer. For anaerobic experiments, we made the instrument anaerobic by filling the system with a solution of 30 nM glucose oxidase and 1 mM glucose in anaerobic buffer the night before the experiment was to be conducted. Oxygen was removed from enzyme solutions via application of several cycles of vacuum and oxygen-scrubbed argon, while substrate solutions were bubbled with oxygen-scrubbed argon. To maintain anaerobic conditions, 36 nM glucose oxidase and 5 mM glucose were added to the solutions. To study the reaction of the reduced enzyme with oxygen, 60 $\mu$M enzyme was first mixed anaerobically in the stopped-flow instrument with either 500 $\mu$M spermine or 200 $\mu$M $N^1$-acetylspermine. After an aging time of 300 or 20 ms for spermine or $N^1$-acetylspermine, respectively, the reduced enzyme was mixed with buffer equilibrated with different oxygen concentrations. The concentration of substrate used and the delay time before the second mix were selected to minimize the excess of substrate while ensuring that formation of the reduced enzyme−product complex was at least 90% complete before the second mix. For pH profiles, the buffers were 200 mM PIPES from pH 6.0 to 6.8, 200 mM Tris-HCl from pH 7.0 to 8.5, and 200 mM CHES from pH 9.0 to 10.0. All rapid-reaction experiments with spermine as the substrate were conducted at 25 °C, while those with $N^1$-acetylspermine were conducted at 4 °C.

*Data Analysis*. Kinetic data were analyzed using KaleidaGraph (Adelbeck Software, Reading, PA). Single-value decomposition of diode array detector data to yield the flavin spectra of intermediates was conducted using the program Sfit (Biologic Science Instruments, Grenoble, France). The Michaelis−Menten equation was used to determine $k_{cat}$, $k_{cat}/K_M$, and $K_M$ values when initial rates were measured as a function of the concentration of a single substrate. Equation 1 was used to analyze inhibition data

$$\frac{v_0}{E} = \frac{k_{cat}S}{K_M\left(1+\frac{I}{K_{is}}\right)+S\left(1+\frac{I}{K_{ii}}\right)} \quad (1)$$

where $K_{is}$ is the inhibition constant determined from the effect of the inhibitor on the $k_{cat}/K_M$ value (slope) and $K_{ii}$ is the inhibition constant determined from the effect on the $k_{cat}$ value (intercept). Equation 2 was used to analyze the pH dependence of kinetic parameters that decreased at both low and high pH.

$$\log Y = \log\left(\frac{C}{1+\frac{H}{K_1}+\frac{K_2}{H}}\right) \quad (2)$$

Equation 3 was used to analyze the pH dependence of kinetic parameters that decreased only at low pH.

$$\log Y = \log\left(\frac{C}{1+\frac{H}{K_1}}\right) \quad (3)$$

In these equations, $K_1$ and $K_2$ are the dissociation constants for the ionizable groups and $C$ is the pH-independent value of the kinetic parameter of interest. For rapid-reaction studies of enzyme reduction, rate constants were obtained from the change in the visible absorbance of the flavin with time by fitting the data with eq 4, which describes a biphasic exponential decay.

$$A = A_\infty + A_1 e^{-\lambda_1 t} + A_2 e^{-\lambda_2 t} \quad (4)$$

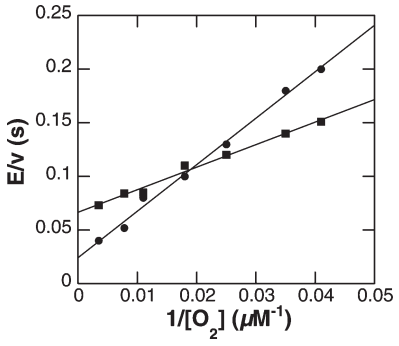


FIGURE 1: Double-reciprocal plot of the initial rate of amine oxidation as a function of oxygen concentration with spermine (●) or $N^1$-acetylspermine (■) as the substrate when the concentration of the amine is fixed at twice the oxygen concentration. Conditions: 25 °C, 0.2 M CHES, and pH 9.0 for $N^1$-acetylspermine and pH 9.35 for spermine.

where $\lambda_1$ and $\lambda_2$ are the first-order rate constants for each phase, $A_1$ and $A_2$ are the absorbances of each species at time $t$, and $A_\infty$ is the final absorbance. The resulting pseudo-first-order rate constants were analyzed using eq 5

$$k_{obs} = \frac{k_2 S}{K_d + S} \quad (5)$$

where $k_2$ is the rate constant for flavin reduction at saturating concentrations of the amine substrate and $K_d$ is the apparent dissociation constant for the substrate. The pseudo-first-order rate constants for oxidation of the reduced enzyme were obtained by fitting the change in absorbance of the flavin with time to eq 6.

$$A = A_\infty + A_1 e^{-\lambda_1 t} \quad (6)$$

The second-order rate constant for oxidation was obtained by fitting the resulting rate constants as a function of the oxygen concentration as a straight line passing through the origin.

## RESULTS

*Kinetic Mechanism of Fms1*. Because spermine and $N^1$-acetylspermine have been reported to be comparable as the best substrates for Fms1 (*11*), the steady-state kinetics of Fms1 with both were examined in some detail. The analyses were conducted at the respective pH optima, 9.3 for spermine and 9.0 for $N^1$-acetylspermine (see below). Flavoprotein oxidases can show either ping-pong or sequential (*24*) steady-state kinetic patterns when the concentrations of both substrates are varied, depending upon whether reduction of the flavin is kinetically reversible (*25*, *26*). For a two-substrate enzyme reaction, the steady-state kinetic pattern can readily be identified using the fixed ratio approach (*27*). In this method, the ratio between the concentrations of the two substrates is kept constant, and the initial rate is determined as a function of the concentration of one of the substrates. Curvature in a double-reciprocal plot suggests a sequential mechanism, while a linear plot arises from a ping-pong mechanism. For Fms1, a double-reciprocal plot of the initial rate versus oxygen concentration at a fixed ratio of either spermine or $N^1$-acetylspermine to oxygen is linear (Figure 1), establishing the kinetic pattern as ping-pong. Fitting these data with the Michaelis−Menten equation gives $k_{cat}$ values of 39.0 ± 1.5 and 15.1 ± 0.4 $s^{-1}$ for spermine and $N^1$-acetylspermine, respectively. Because the fixed ratio approach establishes that the $k_{cat}/K_M$ values for the amine substrate and oxygen are unaffected

Table 1: Steady-State Kinetic Parameters for Fms1 at 25 °C

| substrate | kinetic parameter | value |
|---|---|---|
| spermine[a] | $k_{cat}$[b] | $39.0 \pm 1.5\ s^{-1}$ |
| | $k_{cat}/K_{amine}$[c] | $330 \pm 60\ mM^{-1}\ s^{-1}$ |
| | $K_{amine}$[d] | $118 \pm 25\ \mu M$ |
| | $k_{cat}/K_{O_2}$[e] | $428 \pm 77\ mM^{-1}\ s^{-1}$ |
| | $K_{O_2}$[d] | $91 \pm 16\ \mu M$ |
| $N^1$-acetylspermine[f] | $k_{cat}$[b] | $15.1 \pm 0.4\ s^{-1}$ ($2.5 \pm 0.2\ s^{-1}$ at 4 °C) |
| | $k_{cat}/K_{amine}$[c] | $1400 \pm 200\ mM^{-1}\ s^{-1}$ |
| | $K_{amine}$[d] | $10.9 \pm 1.8\ \mu M$ |
| | $k_{cat}/K_{O_2}$[g] | $358 \pm 20\ mM^{-1}\ s^{-1}$ |
| | $K_{O_2}$[d] | $43.6 \pm 2.3\ \mu M$ |
| $N,N'$-dibenzyl-1,4-diaminobutane[c,h] | $k_{cat}$ | $1.9 \pm 0.08\ s^{-1}$ |
| | $k_{cat}/K_{amine}$ | $1.5 \pm 0.3\ mM^{-1}\ s^{-1}$ |
| | $K_{amine}$ | $1220 \pm 230\ \mu M$ |
| $N,N'$-dibenzyl-1,3-diaminopropane[c,h] | $k_{cat}$ | $0.26 \pm 0.01\ s^{-1}$ |
| | $k_{cat}/K_{amine}$ | $3.4 \pm 0.5\ mM^{-1}\ s^{-1}$ |
| | $K_{amine}$ | $77 \pm 12\ \mu M$ |
| spermidine[c,f] | $k_{cat}$ | $0.87 \pm 0.06\ s^{-1}$ |
| | $k_{cat}/K_{amine}$ | $0.52 \pm 0.1\ mM^{-1}\ s^{-1}$ |
| | $K_{amine}$ | $1660 \pm 340\ \mu M$ |

[a]Determined at pH 9.3. [b]Determined by varying the concentrations of both oxygen and the substrate. [c]Determined at 250 $\mu$M oxygen. [d]The $K_M$ values were calculated from the respective $k_{cat}$ and $k_{cat}/K_M$ values. [e]Determined at 500 $\mu$M spermine. [f]Determined at pH 9.0. [g]Determined with 500 $\mu$M $N^1$-acetylspermine. [h]Determined at pH 9.5.

Table 2: $K_i$ Values for Inhibitors of Fms1[a]

| inhibitor | $K_{is}$ (mM) | $K_{ii}$ (mM) |
|---|---|---|
| 1,12-diaminododecane | $0.05 \pm 0.01$ | $0.28 \pm 0.07$ |
| 1,8-diaminooctane | $0.1 \pm 0.01$ | $0.4 \pm 0.05$ |
| $N,N'$-dibenzyl-1,2-diaminoethane | $0.21 \pm 0.05$ | $1.8 \pm 0.7$ |

[a]Conditions: 250 $\mu$M oxygen, 0.2 M CHES, pH 9.3, and 25 °C.

by the concentration of the other, the individual $k_{cat}/K_M$ values for the substrates and oxygen were determined in separate analyses by varying each at a fixed concentration of the other. The individual $K_M$ values could then be calculated from the respective $k_{cat}/K_M$ and $k_{cat}$ values. For comparison with the rate constants from rapid-reaction analyses, the $k_{cat}$ value with $N^1$-acetylspermine was also determined at 4 °C by varying the concentration of oxygen at a saturating concentration of the amine. The resulting values are listed in Table 1.

To gain further insight into the substrate specificity of Fms1, a number of substrate analogues (Scheme 1) were examined as substrates or inhibitors of the enzyme. While spermidine has been reported not to be a substrate for mammalian SMO or PAO (*15*, *17*), it is a slow substrate for Fms1 at pH 9.0 (Table 1). Several $N,N'$-dibenzyldiamines are either substrates or inhibitors of other polyamine-oxidizing flavoproteins (*17*, *28*). Both $N,N'$-dibenzyl-1,3-diaminopropane and $N,N'$-dibenzyl-1,4-diaminobutane are slow substrates for Fms1 when assayed at the optimal pH for these compounds, pH 9.5 (Table 1). In contrast, $N,N'$-dibenzyl-1,2-diaminoethane is a noncompetitive inhibitor (Table 2). 1,12-Diaminododecane and 1,8-diaminooctane are also noncompetitive inhibitors; the $K_{is}$ and $K_{ii}$ values are provided in Table 2.

*Effect of pH on the Steady-State Kinetic Parameters.* The effects of pH on the $k_{cat}/K_{amine}$, $k_{cat}/K_{O_2}$, and $k_{cat}$ values for spermine and $N^1$-acetylspermine were determined. For both substrates, the $k_{cat}/K_{amine}$−pH profiles are bell-shaped, with maxima of 9.3 and 9.0 for spermine and $N^1$-acetylspermine, respectively (Figure 2). These pH profiles show the importance of two ionizable groups in the free enzyme or substrate. The data

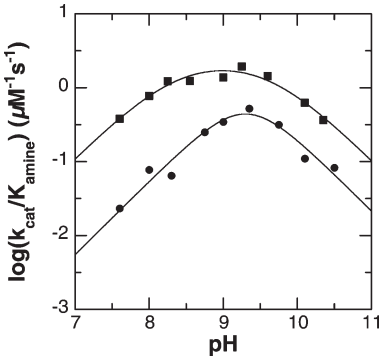


FIGURE 2: Effect of pH on the $k_{cat}/K_{amine}$ value for Fms1 with spermine (●) or $N^1$-acetylspermine (■) as the substrate. The lines are from fits of the data to eq 2.

Table 3: p$K_a$ Values for Fms1[a]

| substrate | kinetic parameter | p$K_1$ | p$K_2$ |
|---|---|---|---|
| spermine | $k_{cat}/K_{amine}$ | $9.3 \pm 0.1$ | $9.3 \pm 0.1$ |
| | $k_{cat}$ | $8.5 \pm 0.1$ | − |
| | $k_{cat}/K_{O_2}$ | $7.51 \pm 0.05$ | − |
| | $k_2$ | $8.30 \pm 0.02$ | − |
| $N^1$-acetylspermine | $k_{cat}/K_{amine}$ | $8.3 \pm 0.1$ | $9.6 \pm 0.1$ |
| | $k_{cat}$ | $7.4 \pm 0.1$ | − |
| | $k_{cat}/K_{O_2}$ | $6.82 \pm 0.05$ | − |
| | $k_2$ | $7.2 \pm 0.1$[b] | − |

[a]Conditions: 25 °C unless otherwise indicated. [b]Determined at 4 °C.

were fit to eq 2 to extract the p$K_a$ values (Table 3). For $N^1$-acetylspermine, the two p$K_a$ values are well-separated; however, with spermine as a substrate, the two p$K_a$ values are too close together to resolve, so that only the average p$K_a$ value of the two ionizable groups can be determined.

With either spermine and $N^1$-acetylspermine as the substrate for Fms1, the $k_{cat}/K_{O_2}$ value is constant at high pH but decreases at low pH (Figure 3), indicating the importance of a single group that must be unprotonated for activity in each case. The data for

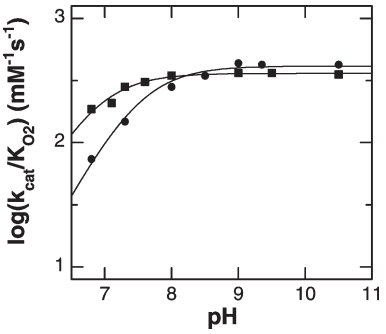


FIGURE 3: Effect of pH on the $k_{cat}/K_{O_2}$ value for Fms1 with spermine (●) or $N^1$-acetylspermine (■) as the substrate. The lines are from fits to eq 3.

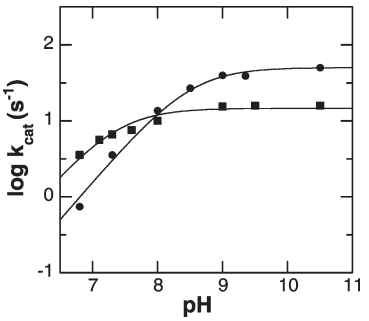


FIGURE 4: Effect of pH on the $k_{cat}$ value for Fms1 with spermine (●) or $N^1$-acetylspermine (■) as the substrate. The lines are from fits to eq 3.

both substrates can be fit to eq 3 to yield the p$K_a$ values listed in Table 3. The $k_{cat}$–pH profiles are shown in Figure 4. With both substrates, the enzyme activity is constant at high pH but decreases at low pH. The data were consequently fit to eq 3 to give the p$K_a$ values listed in Table 3 for the moiety that must be deprotonated for high activity.

Less complete analyses of the effects of pH on the steady-state kinetics of Fms1 with *N*,*N*′-dibenzyl-1,4-diaminobutane and *N*,*N*′-dibenzyl-1,3-diaminobutane as substrates were conducted. With both, the $k_{cat}/K_{amine}$ value was maximal at pH 9.5, decreasing at higher and lower pH (results not shown). Because the activities with both substrates were low even at the pH optimum, more complete analyses were not conducted.

*Rapid-Reaction Kinetics*. Stopped-flow methods were used to examine the kinetics of reduction of Fms1 by spermine and $N^1$-acetylspermine. In initial experiments, the reaction when Fms1 was mixed with either substrate in the stopped-flow spectrophotometer in the absence of oxygen was followed using a diode array detector. The analysis with spermine as a substrate was conducted at 25 °C, while for $N^1$-acetylspermine at this temperature, most of the reaction was complete within the dead time of the instrument; decreasing the temperature to 4 °C slowed the reaction with this substrate sufficiently that it could be followed. For both substrates, the decrease in absorbance upon mixing enzyme with substrate was biphasic, with most of the absorbance change occurring in the much more rapid first phase. To obtain the spectra of the individual species, the spectra as a function of time were analyzed globally as a two-step irreversible reaction using the program Sfit. The resulting spectra with $N^1$-acetylspermine are shown in Figure 5; those for spermine are similar. The visible absorbance spectrum of Fms1 in the absence of substrate is different from that of the species formed in the dead time of the

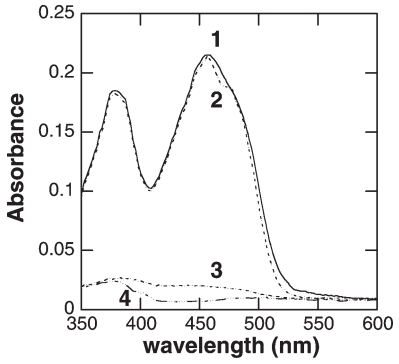


FIGURE 5: Absorbance spectra of flavin intermediates observed in the reductive half-reaction of Fms1 (18 $\mu$M) with 1 mM $N^1$-acetylspermine at pH 9.0 and 4 °C: (1) spectrum of Fms1 in the absence of substrate, (2) spectrum of the initial complex of oxidized enzyme and substrate, (3) spectrum at the end of the first phase, and (4) final spectrum. Spectra 2–4 were obtained by single-value decomposition of the complete spectra as a function of time using the program Sfit and a two-step irreversible kinetic mechanism.

Scheme 3

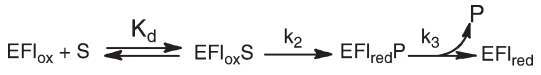


Table 4: Intrinsic Kinetic Parameters for Fms1[a]

| kinetic parameter | value with spermine[b] | value with $N^1$-acetylspermine[c] |
|---|---|---|
| $K_{amine}$ | 24.3 ± 8.2 $\mu$M | 484 ± 83 $\mu$M |
| $k_2$ | 126 ± 3 $s^{-1}$ | 1410 ± 60 $s^{-1}$ |
| $k_3$ | 4.5 ± 0.1 $s^{-1}$ | 0.42 ± 0.01 $s^{-1}$ |
| $k_4$ | 402 ± 15 $mM^{-1}$ $s^{-1}$ | 204 ± 7 $mM^{-1}$ $s^{-1}$ |
| $k_5$ | 56.5 ± 3.4 $s^{-1}$ | 2.5 ± 0.2 $s^{-1}$ |

[a]At pH 9.0. [b]At 25 °C. [c]At 4 °C.

stopped flow. With either substrate, the latter exhibits a shoulder at ~480 nm, suggesting that it is the oxidized enzyme–amine complex. In contrast, the spectra of the intermediate and final species have little absorbance above 400 nm, establishing that the flavin is reduced in both. These results are consistent with the mechanism of Scheme 3, in which binding of the substrate to the enzyme is followed by the reduction of the flavin and oxidation of the substrate in a single first-order step. The oxidized amine then slowly dissociates from the reduced enzyme.

To obtain the rate constants for the individual steps in Scheme 3, the changes in the flavin absorbance were monitored at 458 nm when the enzyme was mixed with different concentrations of spermine or $N^1$-acetylspermine. With both substrates, only the first-order rate constant for the fast phase is substrate-dependent. The rate constants at different substrate concentrations for this phase could be fit to eq 5. The resulting $k_2$ and apparent $K_d$ values are listed in Table 4. The rate constant for the slow phase ($k_3$ in Scheme 3) has values of 4.5 ± 0.1 and 0.42 ± 0.01 $s^{-1}$ for spermine and $N^1$-acetylspermine, respectively.

The effect of pH on the rate constants for the reductive half-reaction was also determined for both substrates. The $k_2$–pH profiles are shown in Figure 6. With both substrates, the value of $k_2$ is pH-independent at high pH, decreasing at low pH, while the value of $k_3$ is not affected significantly by pH. The data were fit to eq 3 to obtain the p$K_a$ values (Table 3) for the moiety that must be unprotonated for reduction.

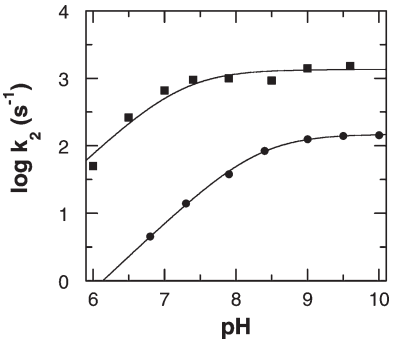


FIGURE 6: Effect of pH on $k_2$, the rate constant for reduction of Fms1, with spermine (●) at 25 °C or $N^1$-acetylspermine (■) at 4 °C. The lines are from fits of the data to eq 3.

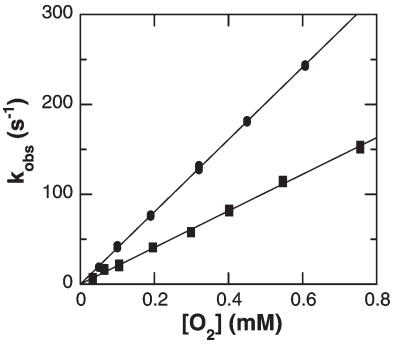


FIGURE 7: Dependence of the rate constant for flavin oxidation at pH 9.0 on the oxygen concentration for the reaction with spermine (●) at 25 °C or $N^1$-acetylspermine (■) at 4 °C.

Stopped-flow spectrophotometry was also used to analyze the kinetics of the reaction of the reduced enzyme−product complex with oxygen. This was done in double-mixing experiments in which Fms1 was first mixed with the amine substrate in the absence of oxygen and allowed to react to form the reduced enzyme−product complex. The sample was then mixed with oxygenated buffer and the reaction followed at 458 nm. The absorbance changes as a function of time could be fit as a single-exponential increase in all cases. The resulting pseudo-first-order rate constants vary directly with the oxygen concentration (Figure 7), consistent with an irreversible bimolecular reaction. The second-order rate constant for the reaction of the reduced enzyme with oxygen is $402 \pm 15$ $mM^{-1}$ $s^{-1}$ with spermine and $204 \pm 7$ $mM^{-1}$ $s^{-1}$ with $N^1$-acetylspermine as the amine substrate.

## DISCUSSION

The results presented here establish the kinetic mechanism of Fms1 and provide insight into the substrate specificity of this enzyme. The results of the kinetic analyses of Fms1 described here are consistent with the kinetic mechanism of Scheme 4 and the values for the individual rate constants given in Table 4. The ping-pong steady-state kinetic pattern for Fms1 with either spermine or $N^1$-acetylspermine (Figure 1) can be attributed to reduction of the flavin ($k_2$ in Scheme 4) being kinetically irreversible, so that binding of the amine and the binding of oxygen are separated by an irreversible step (*25*). The rapid-reaction analyses provide the values of the individual rate constants. The analyses of the reductive half-reaction yield the $K_d$ value for binding of the substrate to the oxidized enzyme ($EFl_{ox}$), the first-order rate constant for reduction, $k_2$, and the rate constant for the release of product from the reduced enzyme−product complex ($EFL_{red}P$), $k_3$. The rate constant for oxidation of the reduced enzyme−product complex, $k_4$, is from the double-mixing stopped-flow experiment, and the rate constant for release of the product from the oxidized enzyme−product complex ($EFl_{ox}P$), $k_5$, can be calculated.

The changes in the absorbance spectrum of Fms1 (Figure 5) when it is mixed with either spermine or $N^1$-acetylspermine in the absence of oxygen are consistent with the kinetic mechanism of Scheme 3. Binding of the substrate to the enzyme occurs within the dead time of the stopped-flow instrument (~1.5 ms). The shoulder at ~475 nm in the visible absorbance spectrum of the enzyme−substrate complex is consistent with spectral changes seen with other amine-oxidizing flavoproteins upon binding the substrate (*29*, *30*). Reduction of the flavin in Fms1 and oxidation of the substrate occur in a single first-order step, with no evidence of intermediates. The mechanism of amine oxidation by members

Scheme 4

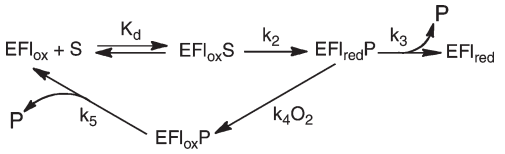


of the MAO family has been a matter of controversy (*22*, *31*, *32*). Proposed mechanisms involving a radical intermediate or nucleophilic attack of the amine substrate on the flavin C4a position involve intermediates that should be detectable during the reductive half-reaction because of their distinct spectral properties. In contrast, a direct hydride transfer mechanism, supported by measurement of deuterium and $^{15}N$ kinetic isotope effects (*30*, *33*), does not involve such an intermediate. Spectral changes consistent with the formation of a flavin radical or a substrate−flavin adduct have generally not been observed during the reduction of members of the MAO/PAO family (*16*, *17*, *30*, *34*, *35*), and our results with Fms1 are in line with that observation.

In the oxidative half-reaction of Fms1, the reaction of the reduced enzyme−product complex with oxygen occurs in a single pseudo-first-order process with no detectable intermediates. Kinetically, with both substrates, the reaction behaves as a simple second-order reaction, with a rate constant equal to the $k_{cat}/K_{O_2}$ value determined from the steady-state analysis. This agreement establishes that oxidation of both spermine and $N^1$-acetylspermine includes only one path for the reaction of the reduced flavin intermediate with oxygen. The reaction of reduced flavins with oxygen is generally thought to proceed by an initial outer sphere electron transfer to form the flavin semiquinone and superoxide followed by rapid electron transfer to form either $H_2O_2$ and oxidized flavin or a flavin 4a-hydroperoxide (*36*−*38*). Neither intermediate is typically seen in the oxidation of a flavoprotein oxidase, with the exception of the recent observation of a flavin 4a-hydroperoxide in the reaction of a pyranose oxidase (*39*).

The rate constant for product release ($k_5$) was not measured directly. However, it is possible to calculate the value of this rate constant. The $k_{cat}$ value contains all the first-order rate constants in the reaction. The only first-order rate constants in the mechanism of Scheme 4 are $k_2$ and $k_5$, so that $k_{cat}$ is described by eq 7.

$$k_{cat} = \frac{k_2 k_5}{k_2 + k_5} \quad (7)$$

Because the $k_{cat}$ and $k_2$ values for both substrates were determined, the value of $k_5$ can be calculated as $56.5 \pm 3.4$ $s^{-1}$ for

spermine at 25 °C and 2.5 ± 0.2 $s^{-1}$ for $N^1$-acetylspermine at 4 °C. With both substrates, the value of $k_5$ is smaller than that of $k_2$, the rate constant for amine oxidation, establishing product release as rate-limiting for Fms1. The relative $k_{cat}/K_{amine}$ values for the two substrates establish that Fms1 has a slight preference for $N^1$-acetylspermine over spermine as a substrate. However, the $k_{cat}$ value for the latter is larger because of the more rapid release of the oxidized amine from the enzyme at the end of the catalytic cycle.

The $k_{cat}/K_{amine}$−pH profiles for Fms1 (Figure 2) are consistent with the enzyme being most active with forms of both spermine and $N^1$-acetylspermine in which two of four nitrogens are protonated. For spermine, the concentrations of the mono-, di-, and triprotonated forms are maximal at pH 10.5, 9.5, and 8.4, respectively, while for $N^1$-acetylspermine, their concentrations are maximal at pH 10.3, 9.0, and 7.0, respectively (*16*). The expected pH distributions of the diprotonated forms agree well with the pH optima in the $k_{cat}/K_M$−pH profiles for spermine of 9.3 and $N^1$-acetylspermine of 9.0. For oxidation of an amine by a flavoprotein, the nitrogen at the site of oxidation must be unprotonated (*16*, *40*). In the case of oxidation of $N^1$-acetylspermine by Fms1, this is N4 (Scheme 1). Because acetylation of N1 prevents it from being protonated, the protonated nitrogens are likely N9 and N12. While these data do not allow unambiguous assignment of the protonation states of the nitrogens in the form of spermine that is the active substrate for SMO, the higher $k_{cat}/K_{amine}$ value for $N^1$-acetylspermine versus spermine establishes that having N1 unprotonated does not result in a poor substrate. Thus, it is likely that in the active form of spermine both N9 and N12 are also charged. The structure of Fms1 with spermine bound (*19*) provides some support for this model. While the structure was determined at pH 5 and therefore represents an inactive complex in which all four nitrogens in spermine are likely fully protonated, it shows a clear interaction between spermine N12[2] and Asp94, consistent with that nitrogen being positively charged. Only weak interactions are seen with N1, and all involve uncharged atoms at 3.6−4 Å; therefore, the neutral nitrogen at this position in $N^1$-acetylspermine could be accommodated.[3]

In the case of mouse PAO, the maxima in the $k_{cat}/K_M$−pH profiles for spermine and $N^1$-acetylspermine correspond to the pH values at which the substrate has a single charged nitrogen (*16*). The pH dependence of a series of spermidine analogues established that the nitrogen that is charged in the form of $N^1$-acetylspermidine that is the active substrate for PAO corresponds to N9 in spermine and $N^1$-acetylspermine. In contrast to the $k_{cat}/K_M$−pH profiles for both Fms1 and PAO, that for spermine as a substrate for human SMO has a maximum at pH 8.3, consistent with an active form of the substrate in which all three of the nonreacting nitrogens are charged (*17*). $N^1$-Acetylspermine is 100-fold worse as a substrate for SMO than is spermine; the inability of N1 to be protonated provides a simple rationale for this substrate preference. Thus, despite similar structures and identical reactions, these three enzymes require differently protonated forms of their common substrates.

The results with the *N*,*N*′-dibenzyldiamine compounds support the conclusion that different requirements for charge in the substrate contribute to substrate specificity in these enzymes. Fms1 will use *N*,*N*′-dibenzyl-1,4-diaminobutane and *N*,*N*′-dibenzyl-1,3-diaminopropane as substrates, with a slight preference for the latter (Table 1). Mouse PAO will also oxidize these compounds with a similar preference, but with $k_{cat}/K_{amine}$ values that are ∼10-fold greater (*28*). In contrast, human SMO has no detectable activity with either compound. The active forms of diamine substrates can have only one protonated nitrogen, because one must be neutral for oxidation. Because PAO prefers the singly protonated form, both compounds are reasonable substrates. They are worse substrates for Fms1, consistent with the lack of a second charged nitrogen. The lack of detectable activity with SMO can be attributed to the lack of two of the three charged nitrogens preferred by that enzyme.

The pH dependence of the inhibition of PAO and SMO by diamines provided further insight into the specificity of those enzymes (*16*, *17*). However, the compounds examined here, 1,12-diaminododecane, 1,8-diaminooctane, and *N*,*N*′-dibenzyl-1,2-diaminoethane, are noncompetitive inhibitors of Fms1. This suggests that they bind to the protein in a different fashion than the substrates. This conclusion is supported by the crystal structures of Fms1 with 1,8-diaminooctane (Protein Data Bank entry 3bi5) or 1,12-diaminododecane (Protein Data Bank entry 3bi5), which show that both compounds bind in the active site tunnel but much farther from the FAD than spermine.

A straightforward explanation for the p$K_a$ seen in the $k_2$−pH profiles for Fms1 with both spermine and $N^1$-acetylspermine is that it is due to N4 of the substrate, which must be neutral for the amine to be oxidized. If the forms of substrates in which N4, N9, and N12 are all protonated can bind but not react, the p$K_a$ for N4 when bound to the enzyme will be seen in this profile. The alternative possibility is that these p$K_a$ values are due to an amino acid residue on the protein. The crystal structure of Fms1 in the complex with spermine (*19*) shows that likely candidates are His67 and His191. Both mouse SMO and human PAO exhibit $k_2$−pH profiles similar to those in Figure 6 (*16*, *17*). With both enzymes, the corresponding p$K_a$ was similarly attributed to N4 in the enzyme−substrate complex. However, in the case of SMO, the effects of pH on the binding of competitive inhibitors implicated an amino acid in binding, suggesting that the p$K_a$ of 7.4 seen in the $k_2$−pH profile for that enzyme could instead belong to a His residue in the active site of the protein (*17*). The present results cannot resolve this ambiguity.

The p$K_a$ seen in the $k_{cat}/K_{O_2}$−pH profiles (Figure 3) depends on the substrate, consistent with it reflecting the need for a moiety in the reduced enzyme−product complex to be uncharged. Mouse PAO shows a p$K_a$ of 7.0 in the $k_{cat}/K_{O_2}$−pH profile with $N^1$-acetylspermine as the substrate (*41*), close to the value of 6.8 described here for Fms1. This p$K_a$ is not seen when Lys315 in PAO is mutated to methionine. While there is no structure of a mammalian PAO available, sequence alignments support Lys315 in mouse PAO as a lysine residue that is conserved in the MAO/PAO family. Structures of several family members show that the amino group of this lysine forms a water-mediated hydrogen bond with N5 of the FAD (*42*, *43*), although this water was not

[2]The numbering used for spermine in Protein Data Bank entry 1xpq and that used here are different. We chose to number the nitrogens in spermine to correspond to the typical numbering in $N^1$-acetylspermine to simplify the comparison between the two substrates. In Protein Data Bank entry 1xpq, the atoms are numbered consecutively from 1 to 14 in the opposite direction from that used here. Thus, N1 as used here corresponds to N14 in the structure file, N4 to N9, N9 to N5, and N12 to N1.

[3]Protein Data Bank entry 3cnd is for the Fms1 complex with $N^1$-acetylspermine. The $N^1$-acetylspermine in that structure does not align with the spermine in Protein Data Bank entry 1xpq, and no atoms of the substrate are within 4 Å of the flavin N5 position. On the basis of these differences, it is likely that the $N^1$-acetylspermine binding mode depicted is not appropriate for catalysis and thus provides limited insight into the structural basis for the substrate specificity of Fms1.

seen in the Fms1 structure (*19*). The results with K315M PAO suggest that the p$K_a$ in the $k_{cat}/K_{O_2}$−pH profile for Fms1 is due to this lysine, Lys296.

Because the $k_{cat}$ value for Fms1 predominantly reflects the rate constant for product release, the pH behavior of the $k_{cat}$ values reported here establishes that the protonation of a group in the oxidized enzyme−product complex decreases the rate constant for release of the product from the oxidized enzyme. A similar pH-dependent release of the oxidized amine product has been described for other flavoproteins that oxidize amines: D-amino acid oxidase (*44*), tryptophan monooxygenase, an L-amino acid oxidase from the MAO structural family (*45*, *46*), and SMO (*41*). Mutating Lys315 in SMO has no effect on the $k_{cat}$−pH profile, ruling out the conserved lysine as the source of the p$K_a$.

In conclusion, the results obtained here provide insight into the catalytic mechanism of Fms1. The complete kinetic mechanism of Fms1 has been determined, and the individual rate constants have been measured. The diprotonated forms of the polyamine substrates are the active forms. Release of product from the oxidized enzyme is rate-limiting for turnover.

## REFERENCES


1. Tabor, C. W., and Tabor, H. (1984) Polyamines. *Annu. Rev. Biochem. 53*, 749–790.
2. Wallace, H. M., Fraser, A. V., and Hughes, A. (2003) A perspective of polyamine metabolism. *Biochem. J. 376*, 1–14.
3. Pegg, A. E. (2009) Mammalian polyamine metabolism and function. *IUBMB Life 61*, 880–894.
4. Casero, R. A., Jr., and Marton, L. J. (2007) Targeting polyamine metabolism and function in cancer and other hyperproliferative diseases. *Nat. Rev. Drug Discovery 6*, 373–390.
5. Wang, Y., and Casero, R. A. (2006) Mammalian polyamine catabolism: A therapeutic target, a pathological problem, or both? *J. Biochem. 139*, 17–25.
6. Seiler, N., Yu, P. M., Tipton, K. F., and Alan, A. B. (1995) Polyamine oxidase, properties and functions. *Prog. Brain Res. 106*, 333–344.
7. Wang, Y., Devereux, W., Woster, P. M., Stewart, T. M., Hacker, A., and Casero, R. A. (2001) Cloning and characterization of a human polyamine oxidase that is inducible by polyamine analogue exposure. *Cancer Res. 61*, 5370–5373.
8. Vujcic, S., Diegelman, P., Bacchi, C. J., Kramer, D. L., and Porter, C. W. (2002) Identification and characterization of a novel flavin-containing spermine oxidase of mammalian cell origin. *Biochem. J. 367*, 665–675.
9. Cervelli, M., Polticelli, F., Federico, R., and Mariottini, P. (2003) Heterologous expression and characterization of mouse spermine oxidase. *J. Biol. Chem. 278*, 5271–5276.
10. White, W. H., Gunyuzlu, P. L., and Toyn, J. H. (2001) *Saccharomyces cerevisiae* Is Capable of *de Novo* Pantothenic Acid Biosynthesis Involving a Novel Pathway of $\beta$-Alanine Production from Spermine. *J. Biol. Chem. 276*, 10794–10800.
11. Landry, J., and Sternglanz, R. (2003) Yeast Fms1 is a FAD-utilizing polyamine oxidase. *Biochem. Biophys. Res. Commun. 303*, 771–776.
12. Chattopadhyay, M. K., Tabor, C. W., and Tabor, H. (2003) Spermidine but not spermine is essential for hypusine biosynthesis and growth in *Saccharomyces cerevisiae*: Spermine is converted to spermidine in vivo by the FMS1-amine oxidase. *Proc. Natl. Acad. Sci. U.S.A. 100*, 13869–13874.
13. Chattopadhyay, M. K., Tabor, C. W., and Tabor, H. (2006) Polyamine deficiency leads to accumulation of reactive oxygen species in a *spe2*Δ mutant of *Saccharomyces cerevisiae*. *Yeast 23*, 751–761.
14. Sebela, M., Radova, A., Angelini, R., Tavladoraki, P., Frebort, I., and Pec, P. (2001) FAD-containing polyamine oxidases: A timely challenge for researchers in biochemistry and physiology of plants. *Plant Sci. 160*, 197–207.
15. Wu, T., Yankovskaya, V., and McIntire, W. S. (2003) Cloning, sequencing, and heterologous expression of the murine peroxisomal flavoprotein, N1-acetylated polyamine oxidase. *J. Biol. Chem. 278*, 20514–20525.
16. Henderson Pozzi, M., Gawandi, V., and Fitzpatrick, P. F. (2009) pH Dependence of a Mammalian Polyamine Oxidase: Insights into Substrate Specificity and the Role of Lysine 315. *Biochemistry 48*, 1508–1516.
17. Adachi, M. S., Juarez, P. R., and Fitzpatrick, P. F. (2010) Mechanistic Studies of Human Spermine Oxidase: Kinetic Mechanism and pH Effects. *Biochemistry 49*, 386–392.
18. Dansen, T. B., Wirtz, K. W. A., Wanders, R. J. A., and Pap, E. H. W. (1999) Peroxisomes in human fibroblasts have a basic pH. *Nat. Cell Biol. 2*, 51–53.
19. Huang, Q., Liu, Q., and Hao, Q. (2005) Crystal structures of Fms1 and its complex with spermine reveal substrate specificity. *J. Mol. Biol. 348*, 951–959.
20. Binda, C., Angelini, R., Federico, R., Ascenzi, P., and Mattevi, A. (2001) Structural bases for inhibitor binding and catalysis in polyamine oxidase. *Biochemistry 40*, 2766–2776.
21. Binda, C., Mattevi, A., and Edmondson, D. E. (2002) Structure-function relationships in flavoenzyme dependent amine oxidations. A comparison of polyamine oxidase and monoamine oxidase. *J. Biol. Chem. 277*, 23973–23976.
22. Fitzpatrick, P. F. (2010) Oxidation of amines by flavoproteins. *Arch. Biochem. Biophys. 493*, 13–25.
23. Whitby, L. G. (1953) New method for preparing flavin-adenine dinucleotide. *Biochem. J. 54*, 437–442.
24. Cleland, W. W. (1963) The kinetics of enzyme-catalyzed reactions with two or more substrates or products. I. Nomenclature and rate equations. *Biochim. Biophys. Acta 67*, 104–137.
25. Palmer, G., and Massey, V. (1968) Mechanisms of flavoprotein catalysis. In Biological oxidation (Singer, T. P., Ed.) pp 263−300, John Wiley and Sons, New York.
26. Porter, D. J. T., and Bright, H. J. (1976) Flavoprotein oxidase mechanisms. In Flavins and Flavoproteins (Singer, T. P., Ed.) pp 225−237, Elsevier Scientific Publishing Co., Amsterdam.
27. Rudolph, F. B., and Fromm, H. J. (1979) Plotting methods for analyzing enzyme rate data. *Methods Enzymol. 63*, 138–159.
28. Henderson Pozzi, M., Gawandi, V., and Fitzpatrick, P. F. (2009) Mechanistic Studies of para-Substituted N,N′-Dibenzyl-1,4-diaminobutanes as Substrates for a Mammalian Polyamine Oxidase. *Biochemistry 48*, 12305–12313.
29. Douzou, P., and Balny, C. (1977) Cryoenzymology in mixed solvents without cosolvent effects on enzyme specific activity. *Proc. Natl. Acad. Sci. U.S.A. 74*, 2297–2300.
30. Ralph, E. C., Anderson, M. A., Cleland, W. W., and Fitzpatrick, P. F. (2006) Mechanistic studies of the flavoenzyme tryptophan 2-monooxygenase: Deuterium and $^{15}N$ kinetic isotope effects on alanine oxidation by an L-amino acid oxidase. *Biochemistry 45*, 15844–15852.
31. Scrutton, N. S. (2004) Chemical aspects of amine oxidation by flavoprotein enzymes. *Nat. Prod. Rep. 21*, 722–730.
32. Edmondson, D. E., Binda, C., and Mattevi, A. (2007) Structural insights into the mechanism of amine oxidation by monoamine oxidases A and B. *Arch. Biochem. Biophys. 464*, 269–276.
33. Ralph, E. C., Hirschi, J. S., Anderson, M. A., Cleland, W. W., Singleton, D. A., and Fitzpatrick, P. F. (2007) Insights into the mechanism of flavoprotein-catalyzed amine oxidation from nitrogen isotope effects on the reaction of N-methyltryptophan oxidase. *Biochemistry 46*, 7655–7664.
34. Miller, J. R., Edmondson, D. E., and Grissom, C. B. (1995) Mechanistic probes of monoamine oxidase B catalysis: Rapid-scan stopped flow and magnetic field independence of the reductive half-reaction. *J. Am. Chem. Soc. 117*, 7830–7831.
35. Gaweska, H., Henderson Pozzi, M., Schmidt, D. M. Z., McCafferty, D. G., and Fitzpatrick, P. F. (2009) Use of pH and Kinetic Isotope Effects to Establish Chemistry as Rate-Limiting in Oxidation of a Peptide Substrate by LSD1. *Biochemistry 48*, 5440–5445.
36. Eberlein, G., and Bruice, T. C. (1983) The chemistry of a 1,5-diblocked flavin. 2. Proton and electron transfer steps in the reaction of dihydroflavins with oxygen. *J. Am. Chem. Soc. 105*, 6685–6697.
37. Massey, V., Schopfer, L. M., and Anderson, R. F. (1988) Structural determinants of the oxygen reactivity of different classes of flavoproteins. In Oxidases and related redox systems (King, T. E., and Mason, H. S., Eds.) pp 147−166, Alan R. Liss, Inc., New York.
38. Roth, J. P., Wincek, R., Nodet, G., Edmondson, D. E., McIntire, W. S., and Klinman, J. P. (2004) Oxygen isotope effects on electron transfer to $O_2$ probed using chemically modified flavins bound to glucose oxidase. *J. Am. Chem. Soc. 126*, 15120–15131.
39. Sucharitakul, J., Prongjit, M., Haltrich, D., and Chaiyen, P. (2008) Detection of a C4a-hydroperoxyflavin intermediate in the reaction of a flavoprotein oxidase. *Biochemistry 47*, 8485–8490.
40. Dunn, R. V., Marshall, K. R., Munro, A. W., and Scrutton, N. S. (2008) The pH dependence of kinetic isotope effects in monoamine oxidase A indicates stabilization of the neutral amine in the enzyme-substrate complex. *FEBS J. 275*, 3850–3858.

41. Henderson Pozzi, M., and Fitzpatrick, P. F. (2010) A lysine conserved in the monoamine oxidase family is involved in oxidation of the reduced flavin in mouse polyamine oxidase. *Arch. Biochem. Biophys. 498*, 83–88.
42. Binda, C., Coda, A., Angelini, R., Federico, R., Ascenzi, P., and Mattevi, A. (1999) A 30 Å long U-shaped catalytic tunnel in the crystal structure of polyamine oxidase. *Structure 7*, 265–276.
43. Binda, C., Li, M., Hubalek, F., Restelli, N., Edmondson, D., and Mattevi, A. (2003) Insights into the mode of inhibition of human mitochondrial monoamine oxidase B from high-resolution crystal structures. *Proc. Natl. Acad. Sci. U.S.A. 100*, 9750–9755.
44. Denu, J. M., and Fitzpatrick, P. F. (1994) pH and kinetic isotope effects on the oxidative half-reaction of D-amino-acid oxidase. *J. Biol. Chem. 269*, 15054–15059.
45. Emanuele, J. J., Jr., and Fitzpatrick, P. F. (1995) Mechanistic studies of the flavoprotein tryptophan 2-monooxygenase. 2. pH and kinetic isotope effects. *Biochemistry 34*, 3716–3723.
46. Sobrado, P., and Fitzpatrick, P. F. (2002) Analysis of the roles of amino acid residues in the flavoprotein tryptophan 2-monooxygenase modified by 2-oxo-3-pentynoate: Characterization of His338, Cys339, and Cys511 mutant enzymes. *Arch. Biochem. Biophys. 402*, 24–30.